PLS multivariate analysis applied to corrosion studies on reinforced concrete

Pablo Monzón[1], José Enrique Ramón-Zamora[1], José Manuel Gandía-Romero[1,*], Manuel Valcuende[2], Juan Soto[1], Daniel Palací-López[3]

[1] The Interuniversity Research Institute for Molecular Recognition and Technological Development (IDM). Polytechnic University of Valencia – University of Valencia. Valencia, Spain.

[2] Department of Architectural Constructions. Polytechnic University of Valencia. Camino de Vera s/n. E-46022, Valencia, Spain.

[3] Multivariate Statistical Engineering Group. Department of Applied Statistics and Operational Research and Quality (DEIOAC). Polytechnic University of Valencia. Camino de Vera s/n. E-46022, Valencia, Spain.

*Corresponding author: José Manuel Gandía-Romero

Email: joganro@csa.upv.es

Telf: 00 34 963877120

Abstract

There are few techniques available to calculate the corrosion rate (i_{corr}) of reinforcing steel in concrete structures. This is due not only to a lack of instrumentation but also because it is necessary to take into account that polarization can irreversibly modify the metal surface and can affect the results or the future state of the metal. This is the reason some researchers prefer to test reinforcing steel with reversible techniques. The main objective of this study is to predict the corrosion rate of reinforced concrete using electrochemical methods combined with statistical tools such as multivariate analysis. Using reinforcements embedded in mortar samples, the corrosion rates were determined at different ages using the Tafel method and values obtained were compared with other techniques: linear polarization resistance (LPR), potentiostatic pulse testing (PPT) and AC electrochemical impedance spectroscopy (EIS). In addition, these values were compared to those obtained using a mixed technique based on

Partial Least Squares (PLS). With this technique, we were able to automatically analyze the current data obtained from LPR, PPT and EIS, and to predict the i_{corr} value. The study allows us to conclude that it is possible to obtain reliable i_{corr} values, very close to those obtained with the Tafel method by using PLS combined with PPT or LPR. Furthermore, it presents several advantages, such as being able to directly treat data without requiring an established Stern-Geary constant (B) for LPR and not having to use an equivalent circuit (EC) in EIS to calculate i_{corr} because only the impedance spectra is necessary.

Keywords: Reinforcing steel, partial least squares (PLS), linear polarization resistance (LPR), potentiostatic pulse technique (PPT), electrochemical impedance spectroscopy (EIS).

1. **Introduction**

Obtaining accurate information about the processes that affect the durability of a reinforced concrete structure is essential because it allows us to determine appropriate intervention or maintenance strategies that might be necessary. Exploring new methods of analysis is useful because reliable information can be obtained, such as that gathered from certain reference methods.

There are several methods to quantify the corrosion process in concrete specimens. Among the most commonly used techniques are the following: Tafel, Linear Polarization Resistance (LPR), Potentiostatic Pulse Testing (PPT), Galvanostatic Pulse Technique and Electrochemical Impedance Spectroscopy (EIS). Tafel extrapolation is one of the more popular methods used to determine corrosion density for activation-controlled corrosion processes. In this method, anodic and cathodic potentiodynamic polarization curves are employed. By using the slope of the linear region of each curve, β_a and β_c can be determined and therefore so can B and i_{corr}. The problem with using this method with concrete is that polarizations greater than 100 mV are applied, which is high enough that it could modify the natural state of the steel surface in

concrete [1]. Once the reinforcing steel is polarized, the specimen needs time to recover its previous E_{corr}.

LPR has become a well-established, simplified method to determine the instantaneous corrosion rate of reinforcing steel in concrete. It is rapid and non-intrusive because low polarizations are applied. Tafel slopes cannot be calculated with this technique so it is necessary to use an established *B* value. For steel reinforcements, it is common to use a *B* value of 26 mV for active corrosion because when in passive state the error is insignificant. This approximation provides a reasonably good estimation of i_{corr} from polarization resistance measurements [2-5].

PPT has been also used to determine i_{corr}. Glass et al. [6] applied potentiostatically induced current transients in order to obtain current density. They achieved this by fitting the current decay with the corresponding equivalent circuit equation. On the other hand, Poursaee [7] determined i_{corr} and *B* by using the results of the potentiostatic transient technique with small polarizations of ± 20 mV, and calculating the area under the current–time curves. Bastidas et al. [8] defined two variants for estimating polarization resistance (*R*p), one from the slope of the plot of ln (ηt) vs. *t* (ηt is the overpotential in volts and *t* the time in seconds) and the other from measuring the time constant of the corrosion process directly. For built structures, galvanostatic pulses are commonly applied in situ with a constant current and the potential response is analyzed [4].

AC electrochemical impedance spectroscopy (EIS) provides information on the steel/concrete system, and from it several parameters can be obtained. It is useful in estimating a steady-state corrosion rate, the dielectric properties of the metal oxide formed on the steel surface, characteristics of the concrete, interfacial corrosion, and mass transfer phenomena [9].

Combining the information obtained via traditional methods and multivariate analysis can be helpful. Chemometrics is defined by the IUPAC (International Union of Pure and Applied Chemistry) as “the science of relating measurements made on a chemical system or process to the state of the system via application of mathematical or statistical methods” [10,11]. In

physics, chemistry, and even in social sciences, multivariate analysis techniques have been widely used. In corrosion, its use is not extensive and only a few examples can be found in the literature [12-15].

In this study, we used Partial Least Squares (PLS) to estimate corrosion density and verify if, by combining this statistical data analysis technique with the data obtained through different electrochemical techniques, it would be possible to predict a reliable corrosion density value that was close to the values obtained by using the Tafel method directly. PLS is an approximation based on the use of latent variables (LV) to find fundamental relationships between the two matrices (X and Y). The X matrix [NxM] is the predictor or input matrix and the Y matrix [NxM] is the output or dependent (response) variables. The LV (few and without correlation) identify underlying causal relationships between X and Y [16-19]. In the field of corrosion science, several processes has been studied using these tools [20-21].

The main objective of this study was to compare the corrosion measured using the Tafel method to the results obtained using other corrosion measurement techniques combined with a statistical model in order to predict the current density. We used several typical non-destructive tests to calculate corrosion values in reinforced concrete structures, including [22]: linear polarization resistance (LPR), potentiostatic pulse testing (PPT) and electrochemical impedance spectroscopy (EIS). A second aim of this study was to use PLS to improve the reliability of the i_{corr} values obtained in concrete corrosion studies. We used the current values obtained in the electrochemical test directly in the PLS matrix. With this technique it is not necessary to establish a *B* value for LPR or an equivalent circuit for EIS.

2. Materials and methods

2.1. Mortar samples and laboratory conditions

The concrete test specimens were subjected to chemically aggressive environments to favor the development of corrosion processes. All the tests were carried out in the laboratory, and the humidity and temperature were controlled to ensure that the exposure conditions were similar.

To perform the tests, we made 12 mortar specimens. The ratio between cement:sand:water was 1:3:0.5, using Ordinary Portland cement (CEM I 42.5) and CEN Standard siliceous sand (according to the European standard En-196-1). In order to obtain four different i_{corr} values, we measured each specimen four times over a year, at 30, 180, 270 and 360 days (48 tests).

We removed all specimens from their moulds 48 hours after concreting, and kept them in the curing chamber at 20ºC and 95% Relative Humidity (R.H.). After 7 curing days, we dried the specimens in the laboratory for 14 days and then immersed them in aqueous solution 0.5M NaCl at 20 ± 5ºC.

All mortar cylinder specimens were made according to the standard UNE 112072:2011 [23]. They were Ø50 mm and 100 mm long, with a 12-mm diameter reinforcing steel rod (B500SD) embedded in the center. The steel rod was sealed with an anticorrosion epoxy coating, RS 199-1468, except at the area where corrosion was going to be monitored. Figure 1 (a) shows the specimen geometry. The steel composition is given in Table 1.

Table 1: Steel composition (%).

C = 0.13	Mn = 0.78	Cu = 0.01	Si = 0.39
P = 0.02	Cr = 0.02	Ni = 0.018	Mo = 0

2.2. Electrochemical techniques

The electrochemical experiments were carried out in a conventional three-electrode thermostated cell (25 ± 1ºC) in a Faraday cage. The counter and reference electrodes were a

stainless steel mesh electrode and a saturated calomel electrode (SCE), respectively, and we used an Autolab PGSTAT 100 (EcoChemie, NL) to control the voltage difference between the two. Figure 1 (b) shows the three-electrode cell design.

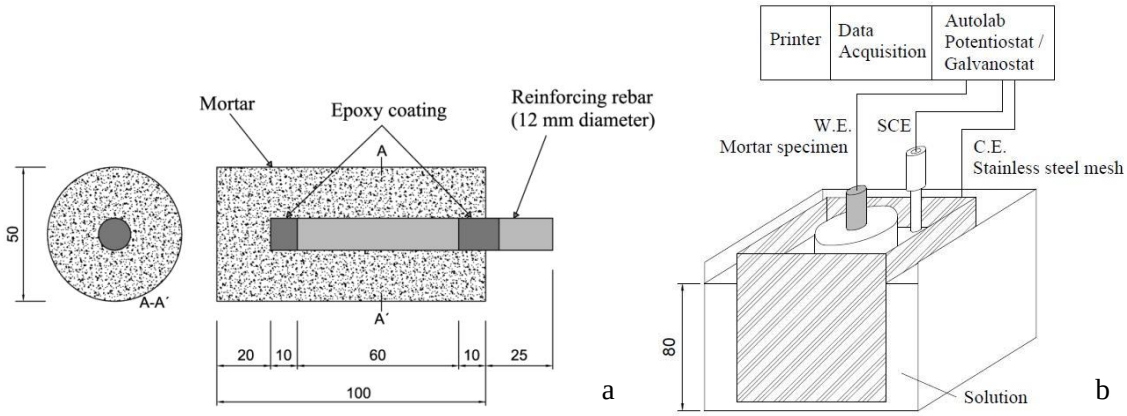

Figure 1: (a) Diagram of mortar specimens. (b) Diagram of the three-electrode cell.

2.2.1. Linear polarization resistance (LPR)

We applied linear polarization resistance (LPR) when the half-cell potentials recorded for the different specimens were stable (we considered E_{corr} to be achieved when the potential drift was less than 0.1 μV/s). For LPR measurements, potential scans began 10 mV below the E_{corr} up to a value of 10 mV at a scan rate of 0.1 mV/s. By applying LPR analysis to the resulting voltammograms, we obtained the *R*p value [23, 24].

Corrosion current density (i_{corr}) is related to *R*p (Ω) through the simplified Stern–Geary equation:

$$i_{corr} = \frac{B}{R_p} \quad (1)$$

where *B* is the Stern–Geary coefficient (related to anodic and cathodic Tafel slopes). As explained in the Introduction section, a *B* value of 26 mV was used for all calculations [5].

2.2.2. Potentiostatic pulse testing (PPT)

After LPR measurement, potentiostatic pulse testing was carried out. When the half-cell potential recorded for each specimen was found to be stable (potential drift less than 0.1 μV/s) we applied the first square wave pulse (+10 mV vs. E_{corr}), and then when the rebar potential was stable again, we applied the second one (-10 mV vs. E_{corr}). The duration of each pulse was 90 seconds. Once the pulse was applied, the area under the current–time curves was used to determine the consumed charge during the polarization process [7]. After tests, Eq. 2 [7] was used to calculate the total consumed charge (Q_{total}) in coulombs.

$$Q_{total} = \int_0^t I \, dt \qquad (2)$$

where t is time (s) and I is current (A). We obtained Q_{total} for both the interfacial corrosion process and the double layer capacitance.

The capacitance (Q_{dl}) obtained through electrochemical impedance spectroscopy is useful to make calculations. For example, by subtracting Q_{dl} from Q_{total}, the charge consumed during the corrosion processes (Q_{corr}) can be calculated and therefore so can i_{corr} (Eq. 3 [7]).

$$Q_{corr} = \Delta Q_{total} - Q_{dl} \qquad (3)$$

2.2.3. Electrochemical impedance spectroscopy (EIS)

We collected EIS test spectra at the corrosion potential (E_{corr}) by using sinusoidal perturbation, an amplitude of ± 10 mV and a sweep from 50000 to 0.010 Hz. The high frequency region (about 10^5 Hz) provides information on the cementitious system [25]. In the middle frequency region (10^4 to 10 Hz), it is possible to study the dielectric properties of a layer formed on the steel surface [26]. In the low frequency region (from a few Hz to a few tenths of a Hz), the EIS spectra are affected by the Faradaic corrosion process occurring on the embedded steel electrodes [27, 28]. To apply this to the study of the corrosion rate of steel reinforcement in concrete, some studies have proposed using B values of 26 mV for the active state and 52 mV for the passive state [23]. These values have also been used in applications of electrochemical

impedance spectroscopy [29]. In our study, however, once Rp (Ω) was obtained with EIS, we calculated i_{corr} using a B value of 26 mV in all cases.

Nyquist and Bode plots show different information like electrode or electrolyte resistance and are a useful way to study the behavior of each corrosion group. Therefore, after taking the PPT measurements, we measured AC impedance and presented the data in the form of Nyquist and Bode plots. We fitted each impedance spectra with its corresponding equivalent circuit (EC) to obtain results for the most important parameters like electrode resistance, mortar resistance and capacity. We used Autolab Nova software to perform the fitting, all the main corrosion values were obtained from the corresponding EC. The proposed circuits are consistent with the circuit used to analyze the electrical response when the potentiostatic pulse method is applied [30]. The 12 specimens measured earliest (30 days) were fit with model A while the rest were fit with model B (Fig. 2).

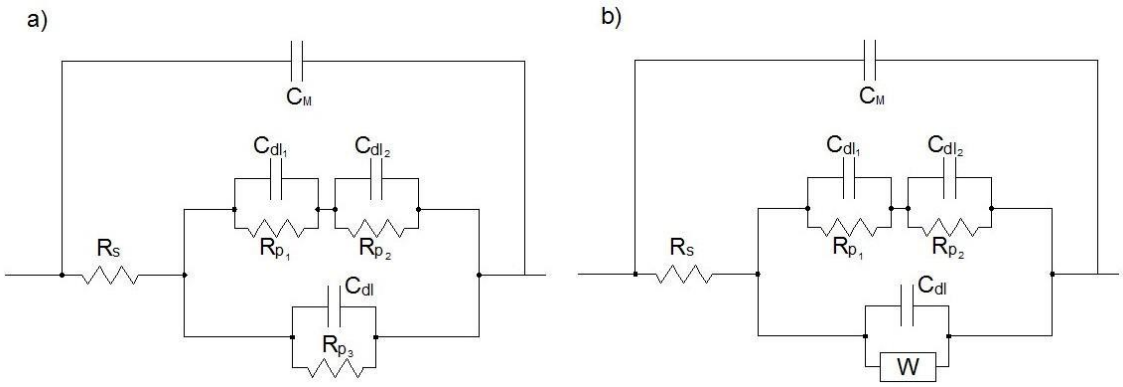

Figure 2: Equivalent circuits (EC) used to fit the experimental spectra.

Figure 2A is a parallel combination with three parts: (1) macroscopic capacitance (C_M), (2) a branch related with the capacity and resistance of the anodic region (oxidation process), and (3) a branch related with the capacity and resistance of the cathodic region (reduction process of the molecular oxygen on the steel surface). R_S is the solution/mortar resistance. The second branch has a serial circuit with two different parts due the Faradaic resistance associated with the oxidation process, Fe^0-Fe^{+2} ($2e^-$) and Fe^{+2}-Fe^{+3} ($1e^-$), and the double layer capacitance for each is C_{dl_2} and C_{dl_1}. The third part includes a capacitance (C_{dl}) and polarization resistance (R_{p_3}). The

only difference in Figure 2B is that instead of an (R_{p_3}) there is a Warburg element (W). These ECs are widely used to calculate the most important corrosion parameters [28, 31].

2.2.4. Tafel extrapolation method

The Tafel extrapolation method allows the current versus potential curves to be analyzed and provides information about the system's features by means of two basic data: the equilibrium potential value and the current value of the electrochemical corrosion. With this method we can obtain different parameters such as corrosion potential (E_{corr}), corrosion current density (i_{corr}), anodic Tafel slope (β_a) and cathodic Tafel slope (β_c). The Rp value is related to the corrosion rate through the Tafel slopes β_a and β_c in the Stern-Geary equation [32-36]:

$$R_p = \frac{\beta_a \cdot \beta_c}{2.303 \cdot i_{corr} \cdot (\beta_a + \beta_c)} \quad (4)$$

After the EIS test, we applied linear potentiodynamic polarization when the half-cell potential recorded from each specimen was found to be stable. In concrete or mortar samples it is advisable to wait 3 days between anodic and cathodic scans to be sure that the steel sample surface is not damaged after being polarized [32]. Because of this, we carried out all tests in two phases: first we applied a potential scan from 140 mV below the E_{corr} value and three days later from OCP to 140 mV above the E_{corr}. In all phases and tests we used a scan rate of 0.5 mV/s.

We plotted the potential against the logarithm of measured current and then extrapolated the linear Tafel segments to the point of intersection to obtain the principal corrosion parameters.

2.3. Chemometric analysis

2.3.1. PLS analysis

In contrast to OLS (Ordinary Least Squares), which assumes the independence of the regressors and suffers from this limitation if this assumption is not true, PLS (Partial Least Squares) is a

data-based statistical analysis method that takes advantage of the correlation between different variables to compress the information. Due to this, PLS also does not require a design of experiments (DOE), since causality can be inferred in the space of the latent variables. In our case, the aim was to use experimental variables such as *X* to predict the i_{corr} (variable *Y*).

With PLS, irrelevant information can be removed by taking into account the correlation that may exist between *X*/*Y* variables. We can do this by transforming them into a reduced number of latent variables (related to the original *X*/*Y* variables, but uncorrelated with each other), thus maximizing the explained covariance between *X* and *Y* variables, as well as the variance of the *X*/*Y* variables themselves. For statistical analysis, we used Solo (version 6.5, Eigenvector Research Inc.) to perform autoscale pre-processing. This method combines centering and standardization transformations [19].

2.3.2. Data matrix

Each technique provided a different matrix size. The Y-matrix was created using the i_{corr} value obtained with the Tafel method (i_{corr}TP), which was used as the reference technique. The X-matrix values came from the data obtained using the different electrochemical methods (current from LPR or PPT and impedance from EIS). Table 2 shows all PLS parameters.

Table 2: PLS model composition.

Regression model	X-matrix				Y-matrix
	Technique	Parameter type	Size	Total variables	
PLS-LPR	LPR	Current (*A*)	48 x 19	912	i_{corr}TP
PLS-PPT	PPT	Current (*A*)	48 x 800	38400	i_{corr}TP
PLS-EIS-*Z*	EIS	*Z* (Ω)	48 x 50	2400	i_{corr}TP
PLS-EIS-*Z*’	EIS	*Z*’ (Ω)	48 x 50	2400	i_{corr}TP
PLS-EIS-*Z*’’	EIS	-*Z*’’ (Ω)	48 x 50	2400	i_{corr}TP

As seen in Table 2, the matrix size varied for each regression model used. For PLS-LPR, the matrix size was 48x19 because there were 48 specimens and 19 current values in the scan. For PLS-PPT, there were 48 specimens and 800 current values were obtained per specimen. Finally, for PLS-EIS there were 50 different frequencies with 3 parameter types: the total impedance value (*Z)*, the real component (*Z*') and the imaginary component (-*Z*'). Because corrosion intensity is proportional to the current intensity but inversely proportional to the system impedance, it is necessary to linearize the *Z*, *Z*' and -*Z*'' matrices. Therefore, the X matrix used to fit the PLS model contained the inverse of all the values (1/z, 1/z´ or 1/z´´).

2.3.3. Calibration-validation model

Multivariate calibration is the process of combining data from several channels in order to overcome selectivity problems, gain new insight and allow automatic outlier detection [21]. In order to validate the PLS, we used a splitting algorithm to separate the whole data set into a calibration set and validation set. Of the two splitting algorithms available in the Solo software we chose the onion method, which automatically keeps both outer and random inner sample covariance and then the user decides what percentage to keep in the calibration set. The algorithm was set to randomly keep 2/3 in the training set and to use the remaining 1/3 as the calibration set.

3. Results and discussion

3.1. Electrochemical measurements

To calculate the variability of the i_{corr} value between the Tafel method and the others, the root mean square error (RMSE) was taken into account. RMSE gives information related with the standard deviation of i_{corr} values and is calculated as follows:

$$\mathrm{RMSE} = \sqrt{\frac{1}{\mathrm{I_m}-1}\sum_{\mathrm{i}=1}^{\mathrm{I_m}}(\mathrm{n}-\mathrm{n_T})^2} \qquad (5)$$

where n is the value measured by the LPR, PPT or EIS methods; n_T is the value measured by the Tafel method and I_m is the number of samples. Another statistical value that helped show i_{corr} variability was R^2. It was calculated using the trend line when the values for each technique studied were compared with Tafel values. Logically, higher RMSE values involve lower R^2 values.

Table 3 shows the root-mean-square error obtained when Tafel values are compared to the other techniques. The results show that the best values were those obtained using the LPR method where the RMSE is smaller.

Table 3: Statistical values for each technique vs Tafel method.

Technique	RMSE
LPR	0.99
PPT	1.35
EIS	1.11

When i_{corr} (LPR, PPT or EIS) are compared to i_{corr} Tafel in Figure 3, the results of i_{corr} (LPR, PPT or EIS) are more accurate if the fit line is close to the one with slope 1. On the other hand, R^2 values give us information about the precision.

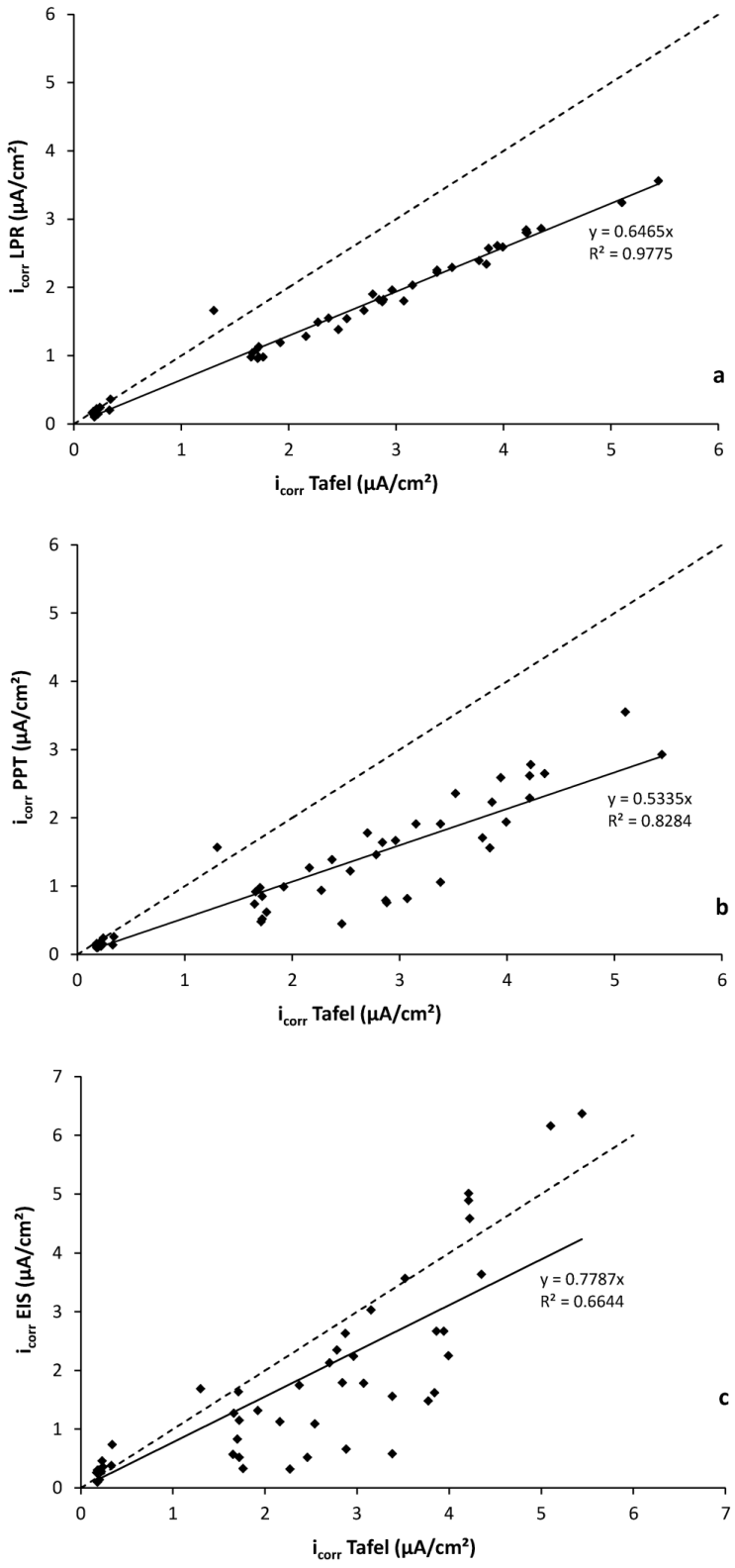

Figure 3: (a) Comparison between i_{corr} obtained with the Tafel method and LPR. (b) Comparison between i_{corr} obtained with the Tafel method and PPT. (c) Comparison between i_{corr} obtained with the Tafel method and EIS.

Figure 3(a) shows results obtained with LPR vs. Tafel. The fit line has a slope of 0.64 and the distribution of points is linear. Therefore, i_{corr} values calculated with LPR were lower than those obtained by Tafel and the error in the prediction was higher when the i_{corr} values increased. The RMSE value was 0.99, which was the smallest value obtained with the different techniques. Taking into account that in LPR technique an established *B* value is used (commonly given a value of 26 mV because the Tafel slopes cannot be calculated), this approximation provides a reasonably good estimation of i_{corr} (maximum error factor of 2). This is evident in the graph because an R^2 value of 0.97 in the fit line shows a high level of precision. If a B value of 40 mV had been used, the slope would be 0.99 and the RMSE 0.23.

On the other hand, Figure 3(b) shows the results obtained with PPT vs Tafel. As before, i_{corr} PPT values were generally lower than those obtained by Tafel, but in this case the average difference between i_{corr} values between methods was higher than before because the RMSE value was 1.35, which was the highest value obtained. Compared with the previous figure, a lower accuracy and lower precision is shown (slope of 0.55 and R^2 of 0.82). In this pulse there are two components, the faradic and non-faradic currents. Therefore, the calculation using the charge integration does not allow the relative importance of each electric component to be discerned. In spite of this fact, PPT is useful because it allows us to evaluate the anodic and cathodic currents in a short time period.

Finally, as seen in Figure 3(c), when i_{corr} obtained using Tafel and EIS were compared, the results showed greater dispersion around i_{corr} values, some of them close to 3 $\mu A/cm^2$. However, the average distance between i_{corr} obtained with Tafel and EIS was smaller than in the previous case. Therefore, the RMSE value was 1.11, an intermediate value between the two previous ones. But it is necessary to take into account that its precision is low in spite of the accuracy given by the slope 0.77x, the one closer to the unit.

3.2. PLS analysis

Once each regression model was obtained, i_{corr} values were predicted through PLS Analysis. All values were calculated with respect to the i_{corr} values measured with the Tafel method. In order to verify the ability of the PLS models to predict i_{corr} values, root mean square error of prediction (RMSEP) was calculated as follows [37]:

$$\mathrm{RMSEP} = \sqrt{\frac{1}{\mathrm{I_p}-1}\sum_{\mathrm{i}=1}^{\mathrm{Ip}}(\mathrm{y_m}-\mathrm{y_{ps}})^2} \quad (6)$$

where y_{ps} is the predicted value for the ith sample from the prediction set, y_m is the measured value for the same sample and I_p is the number of observations in the prediction set.

As previously discussed, the best model for prediction is that for which the fit line is closest to the line with slope 1 (i_{corr}Tafel = 1·i_{corr}(LPR, PPT or EIS)). Due to this definition, RMSE and RMSEP were the same in the previous cases, and can be compared with RMSEP calculated with values predicted via PLS.

Table 4 shows the number of latent variables (LV) used to fit each PLS regression model, the X and Y block percentage for the main LVs (LV1 and LV2) and the main statistical values for the calibration and prediction sets. As is usually the case, this table shows that the first latent variable (LV1) in all models explains most of the variance in the X and Y blocks. Table 4 confirms the higher prediction potential of each PLS model because the low values of RMSEP are even smaller than the RMSE values shown in Table 3. Another statistical value studied was Q^2, whose relationship to RMSEP is similar to that of R^2 and RMSE. As shown, higher RMSEP values involved lower Q^2 values.

Table 4: Results and comparison from PLS models.

Models	LV	LV1 (%)		LV2 (%)		Prediction set	
		X block	Y block	X block	Y block	Q^2	RMSEP
PLS-LPR	4	79.14	94.50	20.67	1.09	0.951	0.33
PLS-PPT	3	98.15	84.74	1.13	3.73	0.977	0.23
PLS-EIS-*Z*	5	95.77	74.77	3.27	13.85	0.873	0.53
PLS-EIS-*Z*’	4	96.67	67.03	2.96	13.97	0.858	0.54
PLS-EIS-*Z*’’	4	77.03	77.91	26.06	6.42	0.846	0.57

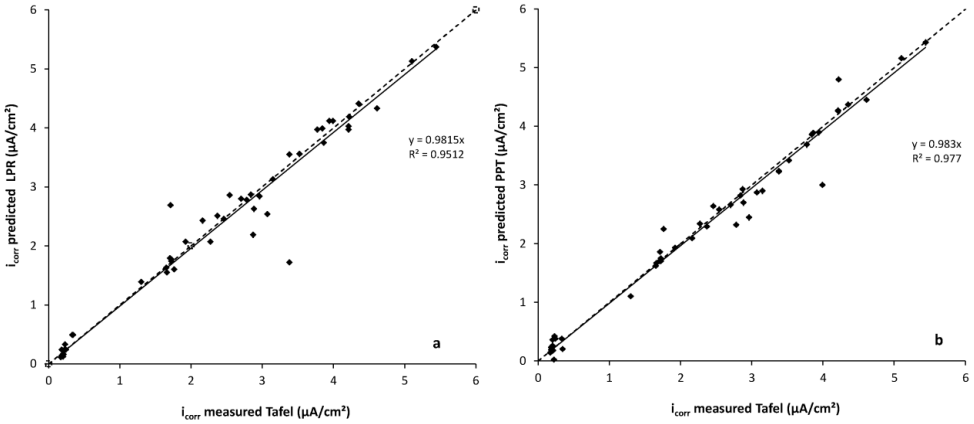

Figure 4 (a) i_{corr} predicted with PLS-LPR vs i_{corr} measured with Tafel. (b) i_{corr} predicted with PLS-PPT vs i_{corr} measured with Tafel. (Dashed line represents the line with slope 1).

Figure 4 (a) shows the regression between i_{corr} LRP (linear polarization) and i_{corr} Tafel. The RMSEP value, as shown in Table 4, is 0.33, which is much smaller than the values shown in Table 3. The distribution of points is almost linear and fits a line with slope 1 reasonably well. This indicates that the predicted i_{corr} LPR values are close to i_{corr} Tafel values. This is a good result and allows i_{corr} values to be calculated in solid specimens with a small margin of error. Figure 4 (b) shows the regression between i_{corr} PPT (potentiostatic pulse) and i_{corr} Tafel. The RMSEP value was 0.23, which was also much smaller than the values shown in Table 3. This

value was the smallest value obtained with PLS regression, so the conclusion can be drawn that the combination of PLS and PPT is the best option for calculating i_{corr} in solid specimens.

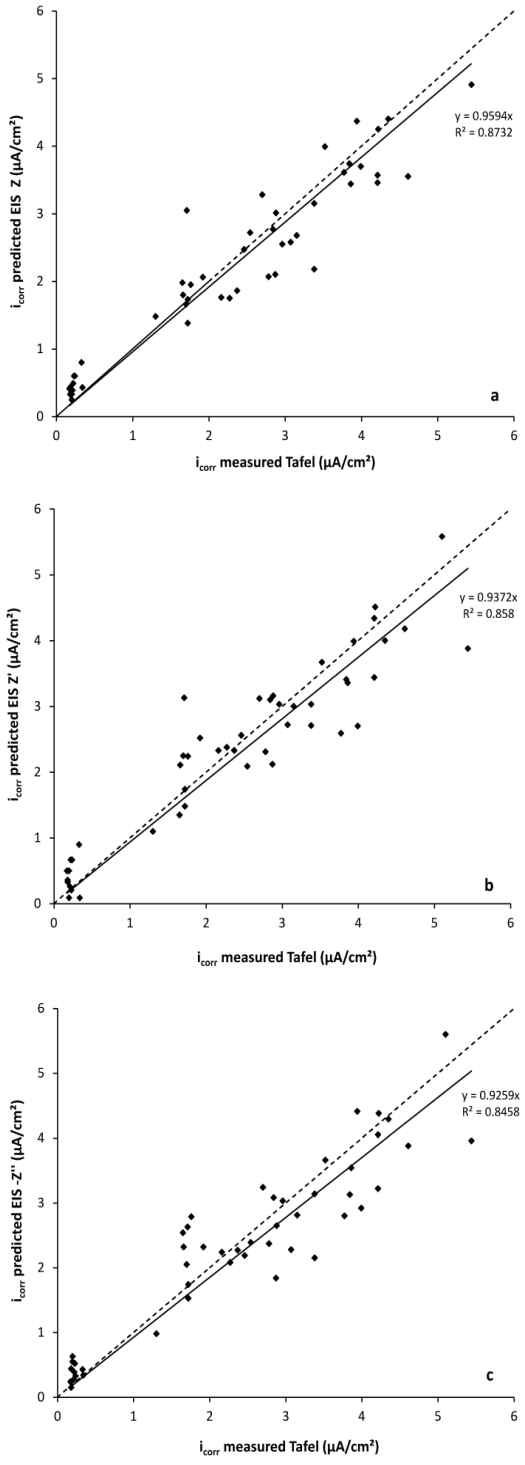

Figure 5 (a) i_{corr} predicted with PLS-EIS (Z) vs i_{corr} measured with Tafel. (b) i_{corr} predicted with PLS-EIS (Z´) vs i_{corr} measured with Tafel. (b) i_{corr} predicted with PLS-EIS (Z´´) vs i_{corr} measured with Tafel (Dashed line represents the line with slope 1).

Figure 5 (a) shows the regression between i_{corr} EIS (using the inverse value of impedance Z) and i_{corr} TP. The RMSEP value was 0.53, which was also smaller than the values shown in Table 3. This combination is still useful for calculating i_{corr} but the result was worse than that calculated above. Figure 5 (b) shows the regression between i_{corr} EIS (using the inverse value of real component Z') and i_{corr} TP. The RMSEP value was 0.54, which is still less than half the value shown in Table 3. Figure 5 (c) shows the regression between i_{corr} EIS (using the inverse value of imaginary component $-Z$'') and i_{corr} TP. The RMSEP value was 0.57. The regression equation yielded large dispersion and therefore worse results compared to the others.

All the PLS models studied were reliable for calculating i_{corr} from the electrochemical data obtained in tests. The results obtained directly using traditional methods (LPR, PPT and EIS) were worse compared to the i_{corr} value obtained with Tafel because of the higher dispersion and error factors. The study shows that the best results were obtained by using PLS combined with PPT or LPR. With respect to the differences obtained in the results using the different methods without PLS compared to with PLS, it is necessary to take into account, for example, that the analysis of LPR-PLS requires all the intensity data of the curve, while in the LPR technique only the slope of the curve is used as a characteristic parameter to calculate Rp, and subsequently $\underline{i_{corr}}$. In addition, arbitrarily assigning parameter B the value of 26 mV can create a certain level of error when using the LPR technique. In the case of the EIS and PPT methods, it is important to note that the equivalent circuit models used in fitting the experimental data may not be the most appropriate if they do not sufficiently reflect the complexity of the chemical system. On the other hand, all the intensity and impedance values used to fit the PLS model are once again taken into account in the case of PPT-PLS and EIS-PLS, respectively. In any case, for subsequent studies it should be kept in mind that the fitting of the model using PLS, as presented in this paper, implicitly assumes the existence of linear relationships between the variables involved, and therefore this has to be considered if there were reasonable doubt of it not being true in the future.

4. Conclusions

We created a model to predict i_{corr} in mortar specimens using non-destructive tests like LPR, PPT and IES. PLS models may be useful in calculating i_{corr} values close to those obtained via the Tafel method, which can be considered a reference method that produces accurate values.

Only by inserting current density values or the inverse of impedance responses is it possible to predict i_{corr}. Once the model is created, it is possible to calculate new i_{corr} values by performing new non-destructive tests. The study showed the following results:

- The worst results were obtained when i_{corr} was calculated using only electrochemical methods: RMSE (root mean square error) obtained were 0.99, 1.35 and 1.11 when LPR, PPT and EIS were used, respectively.
- The best i_{corr} values were obtained using the PLS-PPT regression model. In this case, the RMSEP (root mean square error of prediction) was 0.23.
- The PLS-LPR regression model was the second best combination with respect to efficiency. With this model the RMSEP was 0.33.
- The PLS-EIS model was the model with lower precision and accuracy. Depending on each variable used Z, Z' or $-Z''$, the RMSEP obtained were 0.53, 0.54 or 0.57, respectively.

This research seems to indicate that the proposed methodology allows us to determine corrosion rates with more precision and accuracy compared to other methods used on a regular basis. Further studies are planned in order to verify the results by performing the same tests on real structures or on samples separate from those used in the present work.

References

[1] Chang ZT, Cherry B. Marosszeky M. Polarisation behaviour of steel bar samples in concrete in seawater. Part 1: Experimental measurement of polarisation curves of steel in concrete. Corros Sci. 2008; 50: 357-364.

[2] Broomfield JP. Techniques to assess the corrosion activity of steel reinforced concrete structures. In: N.S. Berke. E. Escalante. C.K. Nmai and D. Whiting ed. ASTM STP 1276; 1996.

[3] Law DW, Millard SG, Bungey JH. Linear polarisation resistance using a potentiostatic controlled guard ring. NDT&E Int 2000; 33: 15-21.

[4] Andrade C, Alonso C. Corrosion rate monitoring in the laboratory and on-site. Construc Build Mater 1996; 10: 315-328.

[5] Buchanan RA, Stansbury EE. Handbook of Environmental Degradation of Materials: Chapter 4: Electrochemical Corrosion. Second edition. Edit. Myer Kutz. Elsevier Inc; 2012.

[6] Glass GK, Page CL, Short NR, Zhang JZ. The analysis of potentiostatic transients applied to the corrosion of steel in concrete. Corros Sci 1997; 39: 1657-1663.

[7] Poursaee A. Potentiostatic transient technique. a simple approach to estimate the corrosion current density and Stern–Geary constant of reinforcing steel in concrete. Cem Concr Res 2010; 40: 1451-1458.

[8] Bastidas DM, González JA, Feliu S. Cobo A, Miranda JM. A Quantitative Study of Concrete-Embedded Steel Corrosion Using Potentiostatic Pulses. Corrosion 2007; 63: 1094-1100.

[9] Saracimen H, Mohammad M, Quddus A, Shameem M, Barry MS, Effectiveness of concrete inhibitors in retarding rebar corrosion. Cement Concrete Comp 2002; 24: 89-100.

[10] Mardia K, Kent J, Multivariate Analysis. London: Acad. Press; 1989.

[11] Pomerantsev AL, Rodionova OY, Chemometric view on comprehensive chemometrics. Chemometr Intell Lab Syst 2010; 103: 19.

[12] Hajeeh M, Estimating corrosion: a statistical approach. Mater Design 2003; 24: 509.

[13] Luciano G, Traverso P, Letardi P, Applications of chemometric tools in corrosion studies. Corros Sci 2010; 52: 2750.

[14] Polikreti K, Argyropoulos V, Charalambous D, Vossou A, Perdikatsis V, Apostolaki C, Tracing correlations of corrosion products and microclimate data on outdoor bronze monuments by Principal Component Analysis. Corros Sci 2009; 51: 2416.

[15] Queiroz Baddini AL, Pressentin Cardoso S, Hollauer E, Cunha Ponciano Gomes JA. Statistical analysis of a corrosion inhibitor family on three steel surfaces (duplex. super-13 and carbon) in hydrochloric acid solutions. Electrochim Acta 2007; 53: 434.

[16] Wold S, Ruhe A, Wold H, Dunn W, The collinearity Problem in Linear Regression. The Partial Least Squares (PLS), Siam J. Sci. Stat. Comput 1984; 5.

[17] Höskuldsson A. PLSregression methods, J. Chemom. 1988; 2: 211-228.

[18] Wold S, Sjostrom, M. PLS-Regression: A basic tool of chemometrics, Chemom. Intell. Lab. Syst. 2001;58:109-130.

[19] Lee JLS, Gilmore IS, Seah MP. Extract of multivariate analysis terminology from ISO 18115-1 Surface Chemical Analysis – Vocabulary – Part 1: General terms and terms for the spectroscopies. National Physical Laboratory. Teddington. Middlesex. UK; 2010.

[20] Baddini ALQ, Cardoso SP, Hollauer E. Gomes JACP. Statistical analysis of a corrosion inhibitor family on three steel surfaces (duplex. super-13 and carbon) in hydrochloric acid solutions. Electrochem Acta 2007; 53: 434-446.

[21] Luciano G, Traverso P, Letardi P. Applications of chemometric tools in corrosion studies. Corros Sci 2010; 52: 2750-2757.

[22] Song HW, Saraswathy V. Corrosion monitoring of reinforced concrete structures – A review. Int J Electrochem Sci 2007; 2: 1-28.

[23] UNE 112072: Determinación de la velocidad de corrosión de armaduras en laboratorio mediante medidas de la resistencia de polarización; 2001.

[24] ASTM G 102-89: Standard pratice for calculation of corrosion rates and related information from electrochemical measurements; 2010.

[25] Xu Z, Gu P, Xie P. Beaudoin JJ. Application of a.c. impedance techniques in studies of porous cementitious materials-II. Relationship between ACIS behaviour and the porous microstructure. Cem Concr Res 1993; 23: 853-862.

[26] John DG, Searson PC, Dawson JL. Use of AC impedance technique in studies on steel in concrete in immersed conditions. Br Corros J 1981; 102-106.

[27] Trabanelli G, Monticelli C, Grassi V, Frignani A. Electrochemical study on inhibitors of rebars corrosion in carbonated concrete. Cement Concrete Res 2005; 35: 1804-1813.

[28] Andrade C, Soler L, Nóvoa XR. Advances in electrochemical impedance measurements in reinforced concrete. Mat Sci Forum 1995; 192: 843-856.

[29] Chang ZT, Cherry B, Marosszeky M. Polarisation behaviour of steel bar in concrete in seawater. Part 2: A polarization model for corrosion evaluation of steel in concrete. Corr Sci 2008; 50: 3078-3086.

[30] Andrade C, Keddam M, Nóvoa XR, Pérez MC, Rangel CM. Takenouti H. Electrochemical behaviour of steel rebars in concrete: influence of environmental factors and cement chemistry. Electrochim Acta 2001; 46: 3905-3912.

[31] Koleva DA, de Wit JHW, van Breugel K, Lodhi ZF, van Westing E. Investigation of corrosion and cathodic protection in reinforced concrete. J Electrochem Soc 2007; 154: 52-61.

[32] Chang ZT, Cherry B, Marosszeky M. Polarisation behaviour of steel bar in concrete in seawater. Part 1: Experimental measurement of polarization curves of steel in concrete. Corr Sci 2008; 50: 357-364.

[33] Stern M, Geary AL. Electrochemical Polarization: I. A Theoretical Analysis of the Shape of Polarization Curves. J Electrochem Soc 1957; 104: 56.

[34] McCafferty E. Validation of corrosion rates measured by the Tafel extrapolation method. Corros Sci 2005; 47: 3202-3215.

[35] Poorqasemi E. Abootalebi O. Peikari M. Haqdar F. Investigating accuracy of the Tafel extrapolation method in HCl solutions. Corros Sci 2009; 51: 1043-1054.

[36] Mansfeld F. Polarisation resistance measurement. Electrochem techn corros 1977; 18-26.

[37] Mariani NCT, Teixeira GHA, de Lima KMG, Morgenstern TB, Nardini V, Júnior LCC. NIRS and iSPA-PLS for predicting total anthocyanin content in jaboticaba fruit. Food Chem 2015; 174: 643-648.